

A chloroplast redox relay adapts plastid metabolism to light and affects cytosolic protein quality control

Valle Ojeda ^{1,*}, Julia Jiménez-López,¹ Francisco José Romero-Campero ¹,
Francisco Javier Cejudo ^{1,*} and Juan Manuel Pérez-Ruiz ^{1,†}

¹ Instituto de Bioquímica Vegetal y Fotosíntesis, Universidad de Sevilla and Consejo Superior de Investigaciones Científicas, Avda. Américo Vespucio 49, 41092-Sevilla, Spain

*Author for communication: fjcejudo@us.es

†Senior author.

‡Present address: California Institute of Quantitative Biosciences, 174 Stanley Hall, Berkeley, CA, USA.

V.O., J.J.-L., and J.M.P.-R. conducted the experiments; F.J.R.-C. analyzed the RNA-Seq data; J.M.P.-R. and F.J.C. designed the experiments; F.J.C. wrote the paper with contributions of all the authors. F.J.C. agrees to serve as the author responsible for contact and ensures communication.

The author responsible for distribution of materials integral to the findings presented in this article in accordance with the policy described in the Instructions for Authors (<https://academic.oup.com/plphys/pages/general-instructions>) is: Francisco Javier Cejudo (fjcejudo@us.es).

Abstract

In chloroplasts, thiol-dependent redox regulation is linked to light since the disulfide reductase activity of thioredoxins (Trxs) relies on photo-reduced ferredoxin (Fd_x). Furthermore, chloroplasts harbor an NADPH-dependent Trx reductase (NTR) with a joint Trx domain, termed NTRC. The activity of these two redox systems is integrated by the redox balance of 2-Cys peroxiredoxin (Prx), which is controlled by NTRC. However, NTRC was proposed to participate in redox regulation of additional targets, prompting inquiry into whether the function of NTRC depends on its capacity to maintain the redox balance of 2-Cys Prxs or by direct redox interaction with chloroplast enzymes. To answer this, we studied the functional relationship of NTRC and 2-Cys Prxs by a comparative analysis of the triple *Arabidopsis* (*Arabidopsis thaliana*) mutant, *ntrc-2cpab*, which lacks NTRC and 2-Cys Prxs, and the double mutant *2cpab*, which lacks 2-Cys Prxs. These mutants exhibit almost indistinguishable phenotypes: in growth rate, photosynthesis performance, and redox regulation of chloroplast enzymes in response to light and darkness. These results suggest that the most relevant function of NTRC is in controlling the redox balance of 2-Cys Prxs. A comparative transcriptomics analysis confirmed the phenotypic similarity of the two mutants and suggested that the NTRC-2-Cys Prxs system participates in cytosolic protein quality control. We propose that NTRC and 2-Cys Prxs constitute a redox relay, exclusive to photosynthetic organisms that fine-tunes the redox state of chloroplast enzymes in response to light and affects transduction pathways towards the cytosol.

Introduction

Redox regulation, based on thiol-disulfide exchange, constitutes a universal regulatory mechanism in which the disulfide reductase activity of thioredoxins (Trxs) plays a key role (Balseira and Buchanan, 2019). Trx activity requires reducing power, which in heterotrophic organisms is provided by NADPH with the participation of an NADPH-dependent Trx

reductase (NTR; Jacquot et al., 2009). In plant chloroplasts, redox regulation plays a key role in the rapid response of photosynthetic metabolism to changes in light intensity (Cejudo et al., 2019; Yoshida et al., 2019; Zaffagnini et al., 2019). However, these organelles present remarkable differences with heterotrophic organisms regarding redox regulation. First, chloroplasts harbor a complex set of up to 20

isoforms of Trxs and Trx-like proteins in clear contrast with the low number of genes encoding either NTRs or Trxs in heterotrophs (Geigenberger et al., 2017; Nikkanen and Rintamaki, 2019). Second, and more importantly, chloroplast Trxs do not rely on NADPH as a source of reducing power, but on photosynthetically reduced ferredoxin (Fdx) with the participation of a Fdx-dependent Trx reductase (FTR; Schürmann and Buchanan, 2008), which links chloroplast redox regulation to light.

The notion that redox regulation in chloroplasts does not rely on NADPH was challenged by the discovery of an NTR with a joint Trx domain at its C-terminus, termed NTRC (Serrato et al., 2004). This enzyme, which shows high affinity for NADPH (Bernal-Bayard et al., 2012), is localized in any type of plant plastids (Kirchsteiger et al., 2012), though it is a relatively abundant protein in the chloroplast stroma (Serrato et al., 2004). Based on the finding that NTRC is a very efficient reductant of 2-Cys peroxiredoxin (2-Cys Prx), a hydrogen peroxide scavenging enzyme, an antioxidant function was proposed for this enzyme (Moon et al., 2006; Pérez-Ruiz et al., 2006; Alkhalifioui et al., 2007). In line with this proposal, several studies have identified the participation of NTRC in plant response to biotic (Ishiga et al., 2012, 2016) and abiotic stresses in plants (Serrato et al., 2004; Chae et al., 2013), green algae (Machida et al., 2012), and cyanobacteria (Sánchez-Riego et al., 2016; Mihara et al., 2017). However, further analyses also showed the participation of NTRC in different redox-regulated processes in plant chloroplasts, which include the biosynthesis of starch (Michalska et al., 2009; Lepistö et al., 2013) and tetrapyrroles (Stenbaek et al., 2008; Richter et al., 2013; Pérez-Ruiz et al., 2014), and the redox regulation of ATP synthase (Carrillo et al., 2016). In addition, mutant Arabidopsis (*Arabidopsis thaliana*) plants devoid of NTRC exhibit inefficient use of light energy (Carrillo et al., 2016; Naranjo et al., 2016a).

The participation of NTRC in such a variety of processes raised the question of the mechanism of action of this enzyme. NTRC contains both NTR and Trx domains (Serrato et al., 2004); hence, it could exert both activities simultaneously. It is well established that NTRC interacts with 2-Cys Prxs through its Trx domain (Pérez-Ruiz and Cejudo, 2009; Bernal-Bayard et al., 2014), therefore, concerning the interaction with 2-Cys Prxs, NTRC could be considered as a Trx bearing its own NTR. Moreover, in vitro assays showed that NTRC is not an efficient reductant of plastidial Trxs (Böhler et al., 2012), suggesting that the enzyme has no NTR activity. However, the overexpression of mutant variants of NTRC (with inactive NTR or Trx domains) partially rescued the phenotype of the Arabidopsis *ntrc* mutant, suggesting that NTRC interacts with chloroplast Trxs, with *f*-type being proposed as the most likely partner of the enzyme (Toivola et al., 2013). The interaction of NTRC with Trx *f*1 was further confirmed by BiFC assays and immunoprecipitation (Nikkanen et al., 2016); this group additionally unveiled the interaction of NTRC with redox regulated enzymes of the Calvin–Benson cycle, such as fructose biphosphatase

(FBPase) and phosphoribulokinase (PRK), and the γ subunit of ATPase (ATPc). In line with these findings, the use of Trx-affinity chromatography confirmed the identification of FBPase as a target of NTRC (Yoshida and Hisabori, 2016); however, no reduction of FBPase by NTRC was detected by in vitro assays (Ojeda et al., 2017). Finally, a double chromatography approach identified additional chloroplast proteins in NTRC-containing complexes (González et al., 2019), thus extending the function of this enzyme to multiple chloroplast processes.

In a previous report (Pérez-Ruiz et al., 2017), we showed that the phenotype of an Arabidopsis mutant lacking NTRC is highly dependent on the total levels of 2-Cys Prxs since the growth inhibition phenotype of the *ntrc* mutant was rescued by decreased contents of these enzymes. Based on these results, we proposed that the redox balance of 2-Cys Prxs, which is maintained by NTRC, controls the activity of the FTR–Trxs pathway. This proposal suggests that NTRC acts via the control of the redox state of 2-Cys Prxs and provides an explanation for the wide variety of processes affected by the absence of this single redox enzyme. However, as stated above, NTRC interacts with different targets, suggesting that it may regulate redox sensitive enzymes in a 2-Cys Prx-independent manner. Thus, the question arising is, what is the actual mode of action of NTRC in chloroplast redox regulation. To address this question, we have generated mutant plants devoid of 2-Cys Prxs A and B (the *2cpab* mutant) and lacking NTRC (the *ntrc-2cpab* mutant). The high similarity of these two mutants, revealed by physiological, biochemical, and transcriptomic analysis, suggests that NTRC exerts a central function on chloroplast redox regulation by an indirect mechanism, which is the maintenance of the redox balance of the 2-Cys Prxs. In addition, the finding of cytosolic chaperones among the most upregulated genes in *2cpab* and *ntrc-2cpab* mutants suggests a relevant function of chloroplast redox homeostasis in cytosolic protein quality control.

Results

The lack of 2-Cys Prxs or NTRC plus 2-Cys Prxs causes very similar phenotypic effects

To analyze the functional relationship of NTRC and 2-Cys Prxs, we have generated a mutant line of Arabidopsis with knockout of both enzymes. We took advantage of the previously reported *2cpab* double mutant (Ojeda et al., 2018a), a knockout for the two 2-Cys Prxs, A and B, present in Arabidopsis, which was manually crossed with the *ntrc* mutant (Serrato et al., 2004) and the triple mutant *ntrc-2cpab* was selected among the progeny. Western blot analysis confirmed the absence of NTRC and 2-Cys Prxs in the *ntrc-2cpab* triple mutant (Figure 1, A and B). The *ntrc-2cpab* plants nearly mimic the phenotype of the *2cpab* mutant in terms of leaf biomass when grown either under short-day (Figure 1, A and C) or long-day conditions (Supplemental Figure S1, A and B). Because the growth phenotype of the *ntrc* mutant is highly dependent on light availability, the

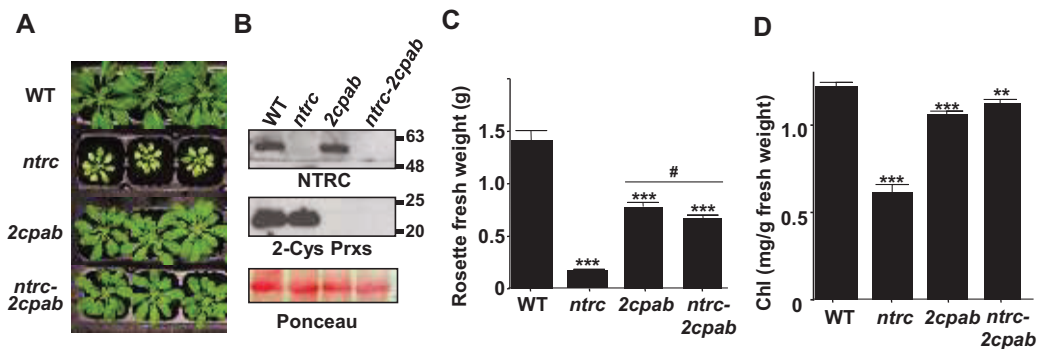


Figure 1 Growth phenotype of Arabidopsis wild-type and mutant lines *ntrc*, *2cpab*, and *ntrc-2cpab* grown under short-day conditions. A, Plants of the wild-type and mutant lines, as indicated, grown under short-day conditions for 7 weeks. B, Western blot analysis of the levels of NTRC and 2-Cys Prxs. Protein extracts were obtained from leaves of plants grown as stated in (A) and subjected to SDS-PAGE under reducing conditions, transferred to nitrocellulose filters and probed with anti-NTRC or anti-2-Cys Prx antibodies. Molecular mass markers (kDa) are indicated on the right. The weight of the rosette leaves (C) and chlorophyll content (D) were determined from at least 25 (C) or 10 (D) plants grown as in (A) and represented as average values \pm SEM. Asterisks represent significant differences compared with the wild-type (** $P < 0.01$; *** $P < 0.001$, Student's *t* test). Hashes indicate significant differences between *2cpab* and *ntrc-2cpab* (# $P < 0.05$, Student's *t* test).

lines under study were challenged with further reduction of the day length by growing plants in a 4-h light/20-h dark regime and light intensity of 125, 400, or 800 $\mu\text{E m}^{-2} \text{s}^{-1}$ (Supplemental Figure S2A). Except for the *ntrc* mutant, which showed a subtle increase of biomass at higher light intensities, the rosette fresh weight of the wild-type, *2cpab*, and *ntrc-2cpab* plants increased with increasing light intensities. Notably, leaf biomass in the *ntrc-2cpab* and *2cpab* mutants was similar and lower than in the wild-type (Supplemental Figure S2, A and B). In line with the above-described growth phenotypes, the high similarity of the *2cpab* and *ntrc-2cpab* mutants was also observed in terms of chlorophyll levels under any of the tested conditions (Figure 1D; Supplemental Figures S1C and S2C). Unlike the *ntrc* mutant, the *ntrc-2cpab* mutant accumulates chlorophyll to similar or slightly increased levels compared to *2cpab* plants (Figure 1D; Supplemental Figures S1C and S2C).

Seedlings of a mutant lacking 2-Cys Prxs were reported to bleach during early developmental stages when grown on sucrose-supplemented medium (Awad et al., 2015), though no quantification of this phenotype was performed. To address the role of NTRC and 2-Cys Prxs during early seedling development, we sought to examine cotyledon phenotype in seedlings with altered levels of these enzymes. Unlike the wild-type and *ntrc* lines, in which nearly all seedlings presented green cotyledons, seedlings from both *2cpab* and *ntrc-2cpab* mutants showed a variety of cotyledon phenotypes from properly developed green to completely albino (Figure 2A). Furthermore, we also observed that seedlings of these mutants displayed defects in pigmentation ranging from pale green, yellowish, or variegated cotyledons, as well as abnormally shaped, asymmetric cotyledons, categorized here in the same class (pale/variegated/asymmetric) for simplicity. Interestingly, the percentage of green (~20%), albino (~50%), and pale/variegated/asymmetric (~30%) phenotypes in seedlings of the *2cpab* mutant was almost

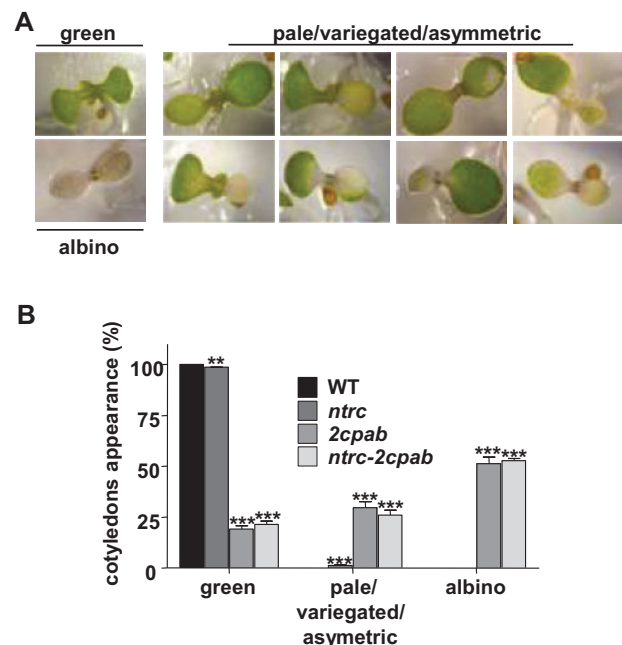


Figure 2 Decreased contents of 2-Cys Prxs affect early stages of plant development. Seedlings of wild-type, *ntrc*, *2cpab*, and *ntrc-2cpab* mutant lines were grown under continuous light (125 $\mu\text{E m}^{-2} \text{s}^{-1}$) on MS synthetic medium supplemented with sucrose. A, Representative cotyledon phenotypes, grouped as green, albino or pale/variegated/asymmetric, of 7-d-old seedlings. B, For each genotype, the percentage of seedlings exhibiting the indicated phenotype was determined and represented as mean values \pm SEM from three independent replicates (sets of at least 50 seedlings). Asterisks represent significant differences compared with the wild-type (** $P < 0.01$; *** $P < 0.001$, Student's *t* test).

indistinguishable of that shown by the *ntrc-2cpab* mutant (Figure 2B). These results suggest that the absence of 2-Cys Prxs, rather than NTRC, is responsible for these seedling phenotypes and extends the similarity between the *2cpab*

and *ntrc-2cpab* mutant lines to early stages of plant development.

For further comparing the phenotypes of the *2cpab* and *ntrc-2cpab* mutants, we analyzed their photosynthetic performance. First, the maximum potential quantum efficiency of photosystem II (PSII), as determined by the F_v/F_m ratio, was more affected in the *ntrc* than in the *2cpab* mutant, which showed F_v/F_m values indistinguishable of those in the *ntrc-2cpab* mutant (Figure 3A). A characteristic feature of the *ntrc* mutant is the inefficient use of light energy as determined by the high nonphotochemical quenching $Y(NPQ)$ at low light intensity (Figure 3B), which is in line with the poor photosynthetic electron transport rate (ETR) at PSII (Figure 3C). Notably, the *2cpab* mutant shows even lower levels of NPQ than the wild-type (Figure 3B) and higher ETR (II) (Figure 3C). Again, these photosynthetic parameters were almost indistinguishable in the *2cpab* and *ntrc-2cpab* mutants (Figure 3, B and C). The efficient light utilization, i.e. lower values of NPQ and higher ETR (II), in the *2cpab* and *ntrc-2cpab* mutants suggests a beneficial effect of the

lack of 2-Cys Prxs on photosynthesis efficiency; however, these mutants showed lower rates of CO_2 assimilation (A_N) than the wild-type at increasing light intensities (Figure 3D). In this regard, it is worth mentioning that mutant plants lacking 2-Cys Prxs show lower stomatal conductance and enhanced stomatal closure (Montillet et al., 2021), indicating the multilevel effect of 2-Cys Prxs on photosynthetic performance. Taken together, these results indicate that the addition of the *ntrc* mutation to plants lacking 2-Cys Prxs results in minor, if any, effect on plant growth and development.

NTRC and 2-Cys Prxs have opposing effects on the redox state of chloroplast enzymes

The functional relationship between NTRC and 2-Cys Prxs was also determined by analyzing the *in vivo* redox state of well-established redox-regulated chloroplast enzymes. Thiol labeling assays by the alkylating agents methyl-maleimide polyethylene glycol (MM-PEG₂₄) or iodoacetamide (IAA) showed full oxidation of the Calvin–Benson cycle enzymes FBPase, PRK, and rubisco activase (RCA) in dark-adapted

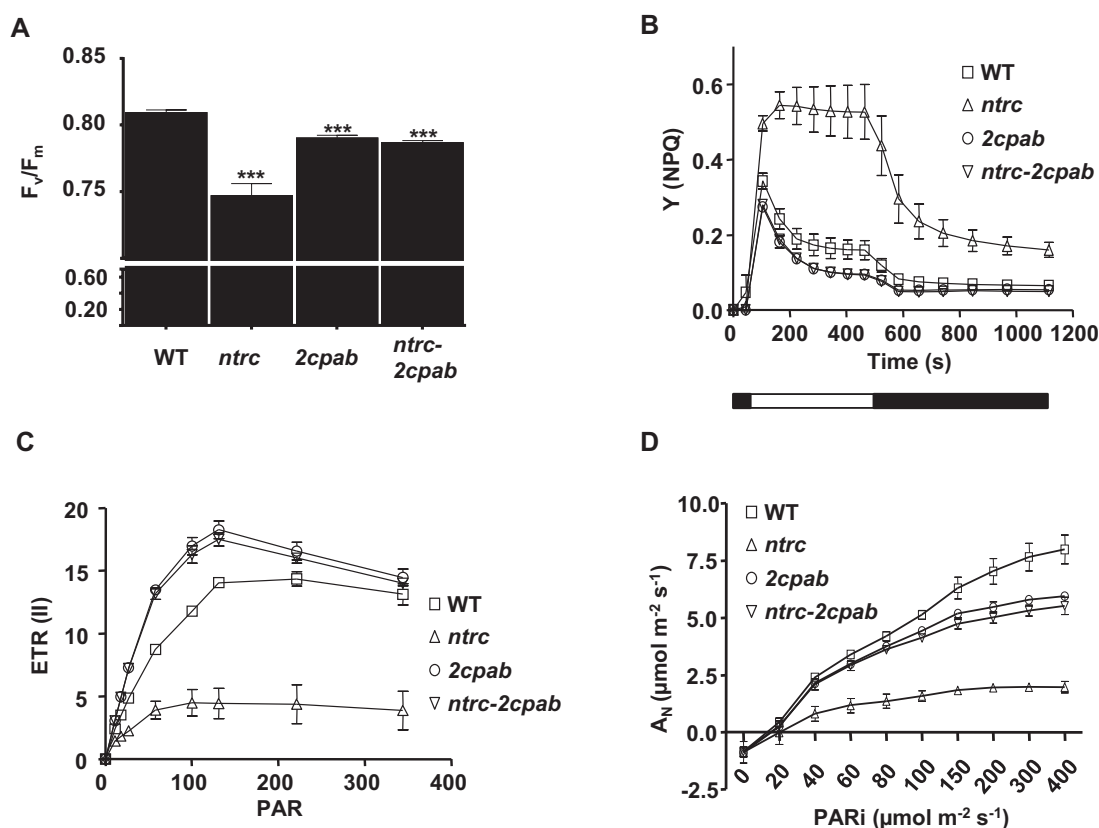


Figure 3 Photosynthetic performance of mutant lines devoid of the NTRC/2-Cys Prx system. Photosynthetic parameters were determined in leaves of plants grown under short-day conditions for 7 weeks. A, The maximum PSII quantum yield was determined as the ratio of variable fluorescence (F_v) to maximal fluorescence (F_m), F_v/F_m , in dark-adapted leaves. The F_v/F_m values ($\pm SEM$) are the average of at least 25 measurements. Statistical significance compared with the wild-type is indicated (***) $P < 0.001$, Student's t test). No significant differences were found between *2cpab* and *ntrc-2cpab*. B, Quantum yields of nonphotochemical quenching, $Y(NPQ)$, were measured in five leaves of plants adapted to darkness, except for *ntrc*, which were performed seven times, and each data point is the mean $\pm SEM$. White and black blocks indicate periods of illumination with actinic light ($75 \mu E m^{-2} s^{-1}$) and darkness, respectively. C, Linear photosynthetic ETR (II), was determined at increasing photosynthetic active radiation (PAR). Each value is the average of five determinations, except for *ntrc* which were performed seven times, and standard errors of the mean (SEM) are represented as error bars. D, Net CO_2 assimilation rate (A_N) was measured using an open gas exchange system in dark-adapted leaves. For each line, three leaves were measured and mean $\pm SD$ are represented.

plants (Figure 4, A, C, and E). In agreement with previous results (Thormählen et al., 2015; Ojeda et al., 2017; Pérez-Ruiz et al., 2017), light-dependent reduction of FBPase (Figure 4, A and B), and PRK (Figure 4, C and D) was severely impaired in the *ntrc* mutant, which also displayed decreased reduction of RCA when compared to the wild-type (Figure 4, E and F). On the contrary, the *2cpab* and *ntrc-2cpab* mutants showed wild-type levels of reduction of PRK (Figure 4, C and D) and even higher reduction of FBPase (Figure 4, A and B) and RCA (Figure 4, E and F). Finally, we evaluated the impact of combined NTRC and 2-Cys Prxs mutations on the redox state of plastid Trxs. To that end,

we selected *f*-type Trxs, which were previously shown to be more reduced in plants overexpressing NTRC (Nikkanen et al., 2016) or those with decreased levels of 2-Cys Prxs (Pérez-Ruiz et al., 2017; Ojeda et al., 2018b). Light-dependent reduction of Trxs *f* was impaired in the *ntrc* mutant as compared to the wild-type, and slightly, but significantly, increased in both *2cpab* and *ntrc-2cpab* mutants (Supplemental Figure S3, A and B). Overall, these analyses indicate a positive effect of the absence of 2-Cys Prxs on the light-dependent reduction of these enzymes.

The function of 2-Cys Prxs in the short-term oxidation of chloroplast enzymes in the dark has been recently reported

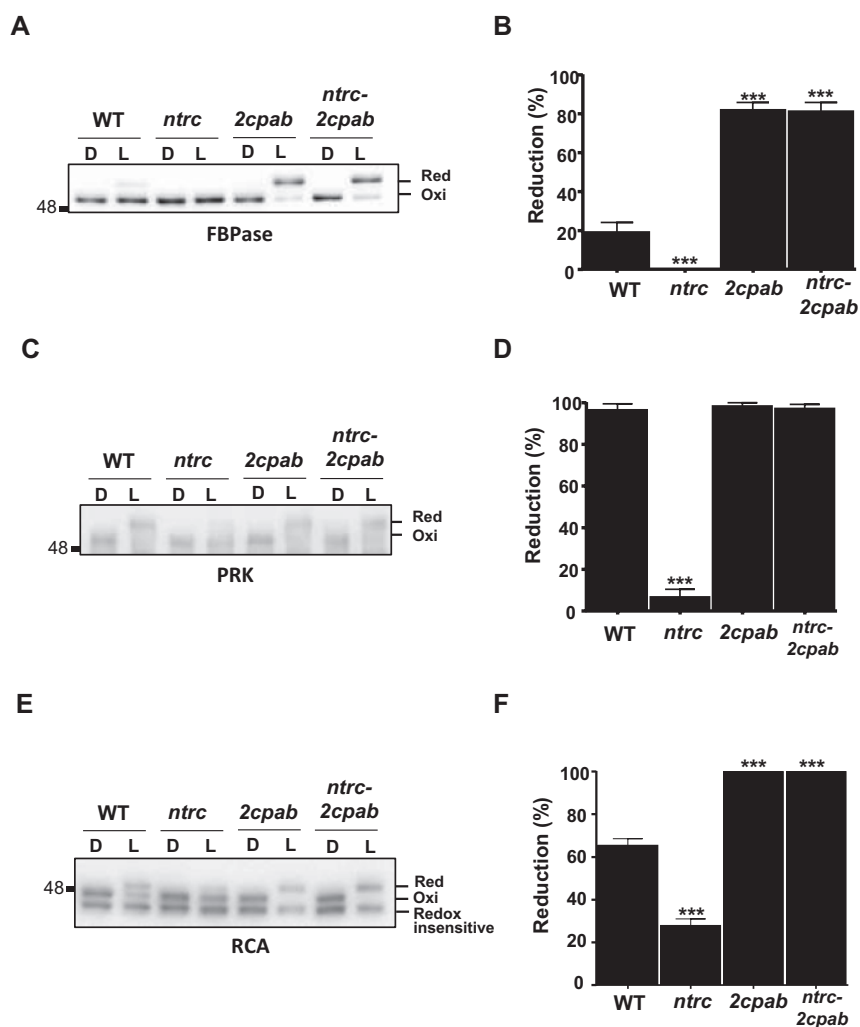


Figure 4 In vivo redox state of FBPase, PRK, and RCA in the *ntrc-2cpab* mutant in response to light. The wild-type and mutant plants were grown under long-day conditions for 4 weeks at a light intensity of $125 \mu\text{E m}^{-2} \text{s}^{-1}$. The in vivo redox state of FBPase (A) PRK (C), and RCA (E) were determined at the end of the dark period (D), and after 30 min of illumination at $180 \mu\text{E m}^{-2} \text{s}^{-1}$ (L) by labeling of the thiol groups with the alkylating agent MM(PEG)₂₄ (A and C) or iodoacetamide (E). Molecular mass markers (kDa) are indicated on the left. Band intensities were quantified (Gel Analyzer) and the percentage of reduction, determined as the ratio between the reduced form and the sum of reduced and oxidized forms, of FBPase (B), PRK (D), and RCA (E) is represented as the mean \pm SEM of four independent experiments. Statistical significance compared with the wild-type is indicated (*** $P < 0.001$, Student's *t* test). No significant differences were found between *2cpab* and *ntrc-2cpab*. Red, reduced; Oxi, oxidized.

(Ojeda et al., 2018a; Vaseghi et al., 2018; Yoshida et al., 2018). In line with this finding, NTRC, which modulates the redox balance of 2-Cys Prxs, also affects the rate of oxidation of chloroplast enzymes in the dark (Ojeda et al., 2018a). To further explore the involvement of the NTRC-2-Cys Prxs system in thiol oxidation, the redox state of FBPase, ATPc, and RCA were analyzed in light-to-dark transitions. The *2cpab* and *ntrc-2cpab* mutants showed indistinguishable and delayed rates of FBPase oxidation in the dark as compared with the wild-type, whereas no significant effect was observed in the *ntrc* mutant (Figure 5, A and B). ATPc and RCA, which are less sensitive to oxidation than FBPase, remained fully and partially reduced, respectively, in the *2cpab* and *ntrc-2cpab* mutants during the time tested (Figure 5, C–F). Interestingly, ATPc oxidation was accelerated in the *ntrc* mutant, which was observed only when 2-Cys Prxs are present (Figure 5, C and D). The positive effect of the lack of NTRC on enzyme oxidation in the dark was further supported by the rate of oxidation of RCA, which was accelerated in the *ntrc* mutant, as compared with the wild-type (Figure 5, E and F). Overall, these results demonstrate the opposing effects of NTRC and 2-Cys Prxs on chloroplast enzyme oxidation.

Global gene expression profiles of the *2cpab* and the *ntrc-2cpab* mutants

Once we established the effects of NTRC and 2-Cys Prxs on plant performance and the redox state of chloroplast enzymes, we analyzed how chloroplast redox control influences the nuclear transcriptome. To that end, we performed a comparative analysis of the *2cpab* and *ntrc-2cpab* genome-wide transcriptomes. RNA sequencing (RNA-Seq) analysis was carried out on three independent biological samples collected from young leaves of both mutant lines and the wild-type. Sequencing quality and absence of contamination were assessed by the high percentage of mapped reads. Scatterplots comparing the expression levels of individual genes between biological replicates showed correlations around 99% (Supplemental Figure S4, A–C). The comparison of the global transcriptomes of the *2cpab* or *ntrc-2cpab* mutants with the wild-type, using a fold change in gene expression of $\pm \log_2(2)$ and $P < 0.05$, identified a remarkably low number of differentially expressed genes (DEGs), 45 and 99 in the *2cpab* and *ntrc-2cpab* mutants, respectively (Figure 6A). The lists of upregulated and downregulated genes in the *2cpab* and *ntrc-2cpab* mutants, as compared to the wild-type, are available as supplemental information (Supplemental Appendix S1). As expected, genes encoding 2-Cys Prxs A and B were among the most downregulated genes in the *2cpab* mutant, and these genes, as well as the NTRC gene were downregulated in the *ntrc-2cpab* mutant, which confirms the consistency of the RNA-Seq analysis data. Of interest, the lack of chloroplast 2-Cys Prxs exerts a remarkable impact in processes taking place outside the organelle, as shown by the subcellular distribution of proteins encoded by DEGs. In the *2cpab* mutant, none of

the 45 DEG, excluding 2-CYS PRXA and 2-CYS PRXB, encodes chloroplast localized proteins (Supplemental Figure S5A). Similarly, genes coding for chloroplast proteins, excluding NTRC and 2-CYS PRX A and B, were also absent in the group of DEGs in *ntrc-2cpab* (Supplemental Figure S5B).

A principal component analysis revealed that the *2cpab* and *ntrc-2cpab* replicates clustered together and separately from the wild-type (Supplemental Figure S6), indicating similar transcriptional profiles between the mutants. Indeed, a substantial percentage ($\sim 73\%$) of DEG in *2cpab* was also differentially expressed in the *ntrc-2cpab* mutant. Thus, of the 28 genes upregulated in the *2cpab* mutant, 20 were also induced in the *ntrc-2cpab* mutant (Figure 6B). Moreover, an additional group of 32 genes specifically upregulated in the *ntrc-2cpab* mutant was detected (Figure 6B). To determine whether these genes constituted truly specific transcriptomic differences between the two mutants, the distribution of their expression fold changes with respect to the wild-type was analyzed (Figure 6C). This analysis revealed that most of the upregulated genes in the *ntrc-2cpab* mutant were also upregulated, although to a lower level, in the *2cpab* mutant, since they exhibit fold changes greater than one. Similarly, most of the downregulated genes in the *2cpab* mutant were also downregulated in the *ntrc-2cpab* mutant (Figure 6D), and most of the 34 genes specifically downregulated in this mutant were also repressed, though to a lower level, in the *2cpab* mutant (Figure 6E), which was confirmed by bar plots showing the expression levels of genes specifically upregulated (Supplemental Figure S7) or downregulated (Supplemental Figure S8) in the mutants. This expression pattern was further verified by reverse transcription quantitative polymerase chain reaction (RT-qPCR) analysis of selected genes (Supplemental Figure S9).

Transcriptomic analysis of the *2cpab* and the *ntrc-2cpab* mutants suggests a role of chloroplast redox homeostasis in cytosolic protein quality control

Gene ontology (GO) term enrichment was performed to obtain a better understanding of the biological processes affected in the *2cpab* and *ntrc-2cpab* mutants (Supplemental Appendix S2). Among the upregulated genes, response to endoplasmic reticulum stress was the most enriched GO term in both mutants (Supplemental Figure S10, A and B). In addition, the GO terms heat-, hydrogen peroxide-, high light-, and oxidative stress-response were specifically enriched in the *2cpab* mutant (Supplemental Figure S10A), whereas GO terms related to biotic stress, such as defense response to pathogens, systemic acquired resistance and salicylic acid biosynthesis, were overrepresented in the *ntrc-2cpab* mutant (Supplemental Figure S10B). Regarding the downregulated genes, no GO term enrichment was found in the *2cpab* mutant, whereas several GO terms related to biosynthesis and metabolism of secondary metabolites containing sulfur (glucosinolates) were significantly enriched in the *ntrc-2cpab* mutant (Supplemental Figure S11).

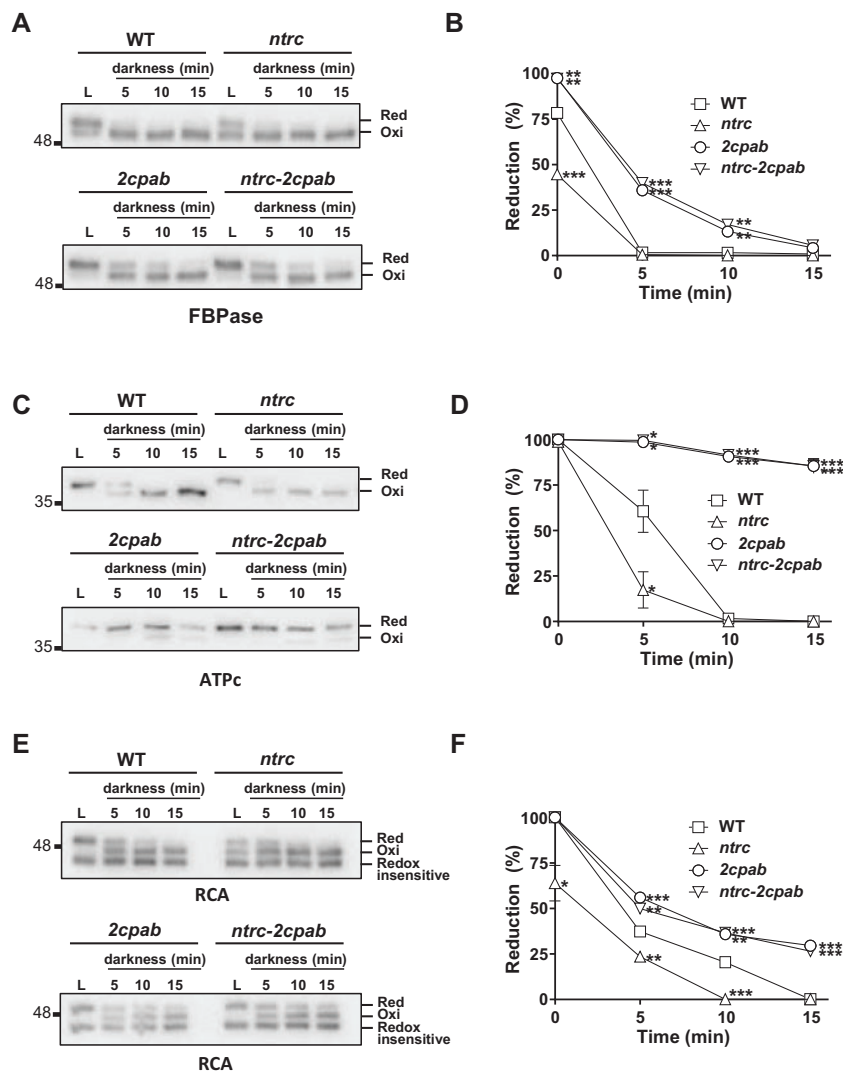


Figure 5 Dark-dependent oxidation of FBPase ATPc and RCA in the wild-type and mutant lines. The wild-type and mutant plants were grown under long-day conditions for 4 weeks at a light intensity of $125 \mu\text{E m}^{-2} \text{s}^{-1}$. At the end of the night period, plants were incubated at a light intensity of $480 \mu\text{E m}^{-2} \text{s}^{-1}$ for 45 min (L); then light was switched off and samples were taken at the indicated times. The *in vivo* redox states of FBPase (A), ATPc (C), and RCA (E) were determined with the alkylating agent iodoacetamide. Molecular mass markers (kDa) are indicated on the left. The corresponding band intensities were quantified (GelAnalyzer) and the percentage of reduction of FBPase (B), ATPc (D), and RCA (F) is shown as the ratio between the reduced form and the sum of reduced and oxidized forms for each protein. Values are the mean \pm SEM of three independent experiments, except for *2cpab* (FBPase and ATPc) where values represent mean \pm SEM of four independent experiments. Statistical significance compared with the wild-type is indicated (* $P < 0.05$; ** $P < 0.01$; *** $P < 0.001$, Student's *t* test). No significant differences were found between *2cpab* and *ntrc-2cpab*. Red, reduced; Oxi, oxidized.

Given the similarity of *2cpab* and *ntrc-2cpab* transcriptomes, we sought to investigate the impact of these mutations in more detail by focusing on genes commonly upregulated and downregulated in both mutants (Supplemental Table S1). Notably, the four most highly induced genes in the *2cpab* mutant, which were also upregulated in the *ntrc-2cpab* mutant, encode heat-shock proteins (HSP), namely HSP70-4, HSP17.6II, HSP23.5, and HSP90-1. In line with this finding, the gene encoding FK506-binding protein 65 (FKBP65), an HSP-interacting co-chaperone (Aviezer-Hagai et al., 2007), was also upregulated, suggesting

impairment of protein quality control in these mutants. Both mutants also displayed increased expression of individual members of the phi class of glutathione transferases (GSTF), *GSTF3*, *GSTF7*, and *GSTF6*, suggesting enhanced oxidative stress in these plants. In addition, several genes commonly downregulated in both mutants were identified, including those encoding the ABA-induced transcription repressor 1 (AITR1), xyloglucan endotransglucosylase/hydrolase 31 (XTH31), and β -amylase 5 (BAM5), which are involved in ABA signaling, cell wall remodeling and starch degradation, respectively. Notably, the *MTO 1 RESPONDING*

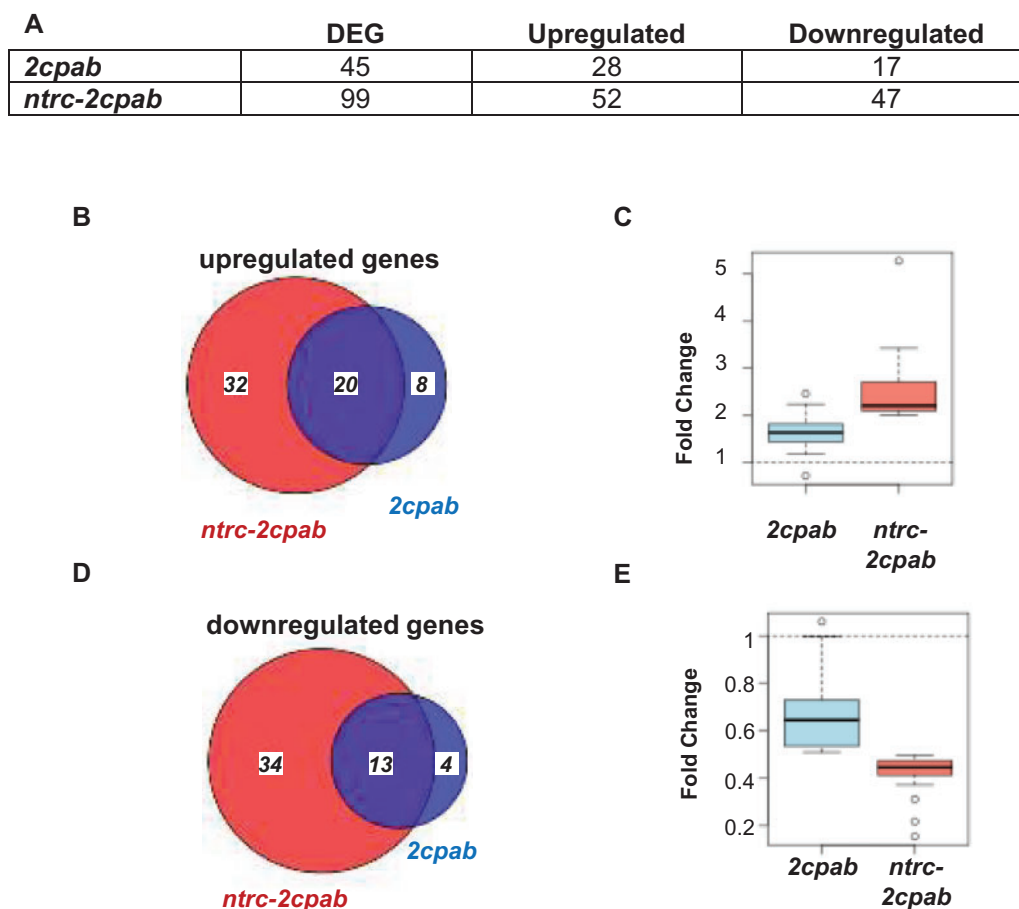


Figure 6 Transcriptome analysis of the wild-type and the *2cpab* and *ntrc-2cpab* mutants. A, Total number of DEG and distribution of upregulated and downregulated genes in the *2cpab* and *ntrc-2cpab* mutants compared to the wild-type (according to a 2-fold change and a *P*-value of 0.05). B–D, Venn diagrams indicating the number of upregulated (B) and downregulated (D) genes in *2cpab* (light blue) and *ntrc-2cpab* (red). The number of genes that overlap among *2cpab* and *ntrc-2cpab* are indicated in dark blue. The fold changes in expression for specifically upregulated (C) and downregulated (E) genes in the *ntrc-2cpab* mutant are represented using boxplots. The median (middle horizontal line), upper and lower quartiles (boxes), as well as minimum and maximum values (whiskers) are indicated. Circles represent high and low extreme values outside 1.5 times the interquartile range (box length) above/below the upper/lower quartile.

DOWN 1 (*MRD1*) gene, with unknown function, showed the highest fold change among the repressed genes. The expression patterns revealed by the transcriptome analysis were confirmed by RT-qPCR analysis on selected upregulated (*HSP17.6*, *HSP23.5*, and *GST7*) and downregulated genes (*MRD1*, *BAM5*, and *XTH31*; Supplemental Figure S12, A and B).

To further explore the impact of the NTRC-2-Cys Prxs redox system on protein quality control, we performed a heat map analysis of individual members of the gene families encoding HSP20s (Supplemental Figure S13A), HSP70s (Supplemental Figure S13B), and HSP90s (Supplemental Figure S13C). Overall, these analyses evidenced that depletion of 2-Cys Prxs, in the presence or absence of NTRC, results in the induction of a specific set of cytosolic chaperones. Of them, we focused on HSP70-4 and HSP90-1 since the levels of these chaperones respond to defective protein import into the chloroplasts (Lee et al., 2009; Wu et al., 2019). Interestingly, the induction of the *HSP70-4* and

HSP90-1 genes, which was validated by RT-qPCR (Figure 7A), was reflected in the levels of their encoded proteins. In the *2cpab* mutant, increased levels of HSP70 (~1.5-fold) and HSP90-1 (~2-fold) were observed relative to the wild-type, whereas slightly higher values were found in *ntrc-2cpab* (Figure 7, B and C). However, it should be noted that contrary to the specific HSP90-1 antibody, the HSP70 antibody recognizes several HSP70 isoforms, likely resulting in an underestimation of HSP70-4 levels in these plants. Overall, these results suggest that redox modulation exerted by 2-Cys Prxs within chloroplasts impact protein quality control systems outside the organelle.

Discussion

Chloroplast 2-Cys Prxs are efficiently reduced by NTRC (Moon et al., 2006; Pérez-Ruiz et al., 2006; Alkhalfioui et al., 2007; Pulido et al., 2010) and, less efficiently, by plastid Trxs (Broin et al., 2002; Collin et al., 2003; Dangoor et al., 2012; Cheng et al., 2014; Eliyahu et al., 2015; Hochmal et al., 2016;

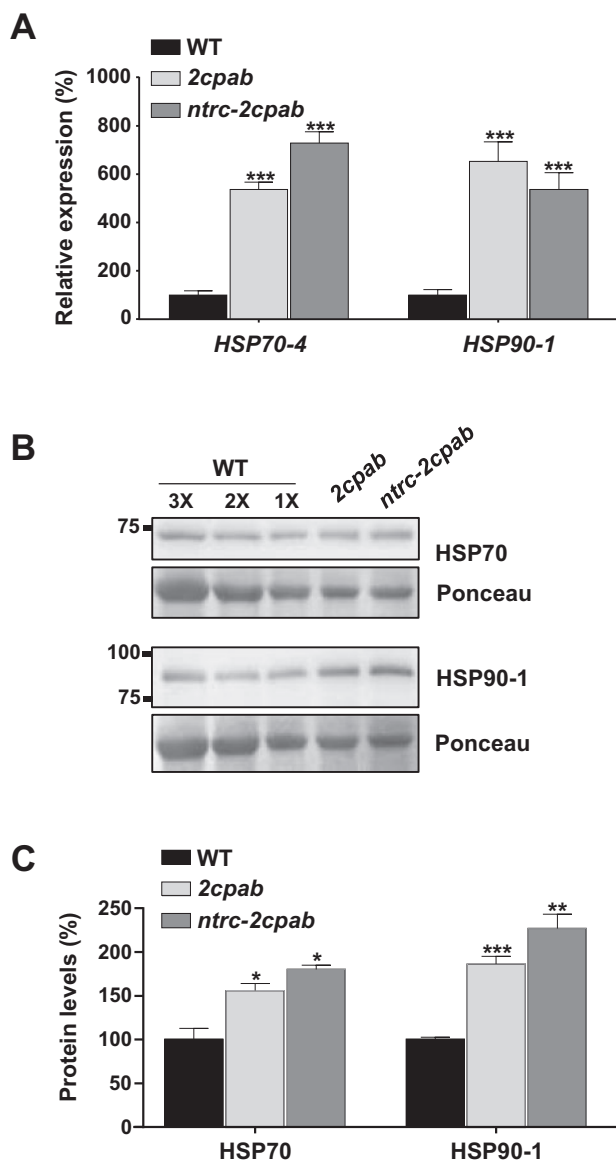


Figure 7 Transcript and protein levels of HSP70-4 and HSP90-1 in the wild-type and the mutants *2cpab* and *ntrc-2cpab*. **A**, Levels of transcripts of HSP70-4 and HSP90-1 were determined by RT-qPCR using RNA isolated from young leaves of plants grown under short-day conditions for 8 weeks. **B**, Western blot analysis of the content of HSP70 and HSP90-1. Protein extracts were obtained from leaves of plants grown as stated in (A) and aliquots of 5 μ g (1X), from all lines, and 10 μ g (2X) and 15 μ g (3X) of WT proteins, as indicated, were subjected to SDS-PAGE under reducing conditions, transferred to nitrocellulose filters, and probed with anti-HSP70 or anti-HSP90-1 antibodies (see methods). Molecular mass markers (kDa) are indicated on the left and even loading was monitored by Ponceau staining of the Rubisco large subunit. **C**, Band intensities corresponding to HSP70, HSP90-1, and Rubisco large subunit were quantified (GelAnalyzer). The contents of HSP70 and HSP90-1, normalized to the levels of Rubisco large subunit, are shown relative to the levels of the WT (1X) sample (arbitrarily assigned a value of 100). Data are given as the mean \pm SEM of three independent experiments. Statistical significance compared with the wild-type is indicated (* $P < 0.05$; ** $P < 0.01$; *** $P < 0.001$, Student's *t* test). No significant differences were found between *2cpab* and *ntrc-2cpab*.

Jurado-Flores et al., 2020), which allows 2-Cys Prxs to modulate the redox state of Trxs in response to changes in light intensity and during the day-night transition (Pérez-Ruiz et al., 2017; Ojeda et al., 2018b). This model suggests a key role for NTRC as the NADPH-dependent master regulator of chloroplast performance and provides an explanation for the ability of the enzyme to modulate different Trx-dependent processes, yet without directly interacting with these targets. However, several approaches, either in vivo (Nikkanen et al., 2016; González et al., 2019) or in vitro (Yoshida and Hisabori, 2016), have identified putative NTRC targets beside 2-Cys Prxs, suggesting that NTRC might exert its activity through the direct interaction with these enzymes. Thus, it remains as an open question whether NTRC acts exclusively via the regulation of 2-Cys Prxs or by interaction with additional targets. In this study, we addressed this issue with a genetic approach based on a comparative analysis of Arabidopsis lines devoid of 2-Cys Prxs (*2cpab* mutant) or NTRC plus 2-Cys Prxs (*ntrc-2cpab* mutant).

Under any of the conditions tested, short-day (Figure 1, A–D), long-day (Supplemental Figure S1, A–C), or ultra-short days (Supplemental Figure S2, A–C), the *2cpab* and *ntrc-2cpab* lines showed very similar growth phenotypes. Therefore, the deficiency of NTRC in Arabidopsis lines that lack 2-Cys Prxs has almost no additional effect, at least in the conditions tested in this work, which supports the notion that NTRC acts exclusively via the regulation of 2-Cys Prxs. A surprising phenotype of the *2cpab* mutant is the aberrant development of seedlings, which show a high proportion of albino and pale/variegated/asymmetric cotyledons when grown on MS medium supplemented with sucrose (Figure 2, A and B). The fact that the *ntrc-2cpab*, but not the *ntrc* mutant, also exhibits this phenotype indicates the participation of 2-Cys Prxs, but not of NTRC, in cotyledon chloroplast biogenesis. On the contrary, at adult stages, the phenotype of the *ntrc* mutant is more severe than that of the *ntrc-2cpab* mutant in all of the conditions tested (Figure 1, A–C; Supplemental Figures S1, A–C and S2, A–C). Therefore, 2-Cys Prxs exert different effects throughout plant development: NTRC-independent at the early stage and NTRC-dependent at the adult stage. A possibility to explain this behavior is that of the two activities, peroxidase and chaperone (Dietz, 2011), displayed by 2-Cys Prx, one could be more relevant for chloroplast biogenesis and the other in mature chloroplasts, but more work is required to test this possibility.

The availability of mutant lines devoid of NTRC and 2-Cys Prxs has allowed us to address the functional relationship of these enzymes in modulating chloroplast redox homeostasis. While the absence of NTRC provokes lower levels of light-dependent reduction of FBPase, PRK, RCA, and Trxs *f*, the absence of 2-Cys Prxs provokes higher levels of reduction, as compared with the wild-type (Figure 4, A–F; Supplemental Figure S3, A–C). However, the rate of oxidation of ATPc and RCA in the dark was accelerated in *ntrc* mutant but delayed

in the *2cpab* mutant (Figure 5, C–F). This effect was not as clear for FBPase (Figure 5, A and B), probably due to the rapid oxidation of this enzyme and its poor light reduction in the *ntrc* mutant. These results indicate that NTRC favors reduction of chloroplast enzymes, and thus their activation in the light, whereas 2-Cys Prxs favor oxidation, hence their inactivation in the dark. Therefore, in absence of NTRC, a decreased reduction of 2-Cys Prxs is expected to increase oxidation of Trxs, consequently lowering the level of reduction of their targets. In the same line of reasoning, the absence of 2-Cys Prxs is expected to decrease oxidation of Trxs, consequently increasing the level of reduction of their targets, in agreement with previously reported data (Perez-Ruiz et al., 2017). The opposing effects of NTRC and 2-Cys Prxs were also observed on photochemical parameters as shown by the lower levels of NPQ and higher ETR (II), respectively, in the *2cpab* and *ntrc-2cpab* mutants (Figure 3, B and C). These results reveal that the NTRC-2-Cys Prxs redox system participates in the concerted regulation of stromal enzymes and photochemical reactions, which might be performed by Trxs. In support of this notion, the Trx *m4*-dependent regulation of photosynthetic cyclic electron transport (Courteille et al., 2013) is exerted via its redox interaction with PROTON-GRADIENT REGULATION 5-LIKE PHOTOSYNTHETIC PHENOTYPE (PGRL1; Okegawa and Motohashi, 2020). The participation of 2-Cys Prxs in enzyme oxidation might be an additional mechanism to dissipate reducing equivalents from reduced stromal enzymes, which might act concertedly with the water–water cycle responsible for photosynthetic control to optimize photosynthetic performance in response to light intensity (Foyer et al., 1990).

As a complementary approach to further explore the functional relationship of NTRC and 2-Cys Prxs, we analyzed the leaf transcriptomes of the *2cpab* and *ntrc-2cpab* mutants. This analysis revealed that depletion of either 2-Cys Prxs or NTRC plus 2-Cys Prxs did not exert a large effect on nuclear gene expression, as shown by the moderate number of DEG identified (Figure 6A). Given the central role proposed for the NTRC-2-Cys Prxs in chloroplast redox homeostasis, these results may be explained by the fact that this analysis was conducted on plants grown under controlled conditions. Thus, more studies under stressful conditions will be required to fully understand the impact of the NTRC-2-Cys Prxs redox system on plant response to the environment. Remarkably, most of the genes upregulated (Figure 6B) or downregulated (Figure 6C) in the *2cpab* mutant were coincident in the *ntrc-2cpab* mutant. Likewise, most of the genes specifically upregulated (Figure 6C; Supplemental Figures S7 and S9) or downregulated (Figure 6D; Supplemental Figures S8 and S9) in *ntrc-2cpab* showed a similar trend in the *2cpab* mutant, supporting the notion that both mutants have similar gene expression profiles, as shown by the principal component analysis (Supplemental Figure S6). Overall, these results demonstrate the high

similarity of the *2cpab* and *ntrc-2cpab* mutants at the transcriptome level.

2-Cys Prxs reduce hydrogen peroxide using thiol-reducing equivalents, hence interconnecting chloroplast antioxidant and redox regulatory mechanisms (Cejudo et al., 2021). In vivo studies showing higher levels of hydrogen peroxide in plants with decreased content of 2-Cys Prxs (Baier et al., 2000; Pulido et al., 2010) support the antioxidant function of these enzymes. In line with this, an Arabidopsis double knock-out mutant lacking both 2-Cys Prxs, A and B, exhibits bleaching in high light, indicating the role of these enzymes in dissipating excess reducing power through the water–water cycle, which protects the photosynthetic apparatus from oxidative stress (Awad et al., 2015). The identification of GO categories of response to heat, hydrogen peroxide, oxidative stress, or light intensity in the *2cpab* mutant (Supplemental Figure S10A) further supports the antioxidant function of 2-Cys Prxs. Moreover, the identification of GO terms related to biotic stress, i.e. defense response to bacterium and fungus or salicylic acid biosynthesis, among the genes overexpressed in the *ntrc-2cpab* mutant (Supplemental Figure S10B), point to redox homeostasis as a relevant component of chloroplast function in plant defense, in line with the well-recognized function of chloroplasts in plant pathogen response (Littlejohn et al., 2021).

Remarkably, response to ER stress was the most enriched GO term among the overexpressed genes of the *2cpab* and *ntrc-2cpab* mutants (Supplemental Figure S10, A and B), whereas DEGs coding for chloroplast localized proteins were absent from both mutants (Supplemental Figure S5, A and B). Thus, the function of 2-Cys Prxs seems to play a relevant role in the signaling function of the organelle, affecting extra-plastidial processes. The predominance of genes encoding cytosolic proteins being among the most upregulated genes, especially in the *2cpab* mutant (Supplemental Figure S5A), uncovers the effect of chloroplast redox homeostasis on the expression of genes encoding proteins not localized in the organelle. In particular, the presence of several cytosolic chaperone proteins among the upregulated genes in both mutants (Supplemental Table S1) indicates that redox impairment within the chloroplast probably affects protein quality control outside the organelle. Heat map analysis showed that, rather than a global effect on chaperone encoding genes, deficiencies of 2-Cys Prxs, or NTRC plus 2-Cys Prxs affect the expression profile of specific isoforms of the HSP20, HSP70, and HSP90 families (Supplemental Figure S13, A–C). The most highly upregulated gene in both mutants encodes the chaperone HSP70-4 (Supplemental Appendix S1 and Supplemental Table S1), whereas remaining isoforms of this family, including the chloroplast-localized HSP70-6 and HSP70-7, showed the wild-type levels of gene expression (Supplemental Figure S13B). Interestingly, a previous study showed that HSP70-4, but not other

HSP70 isoforms, was highly induced in *Arabidopsis* mutants that accumulate chloroplast preproteins, hence playing a role in the proteolytic degradation of these precursors by the 26S proteasome pathway (Lee et al., 2009). Moreover, 2-Cys Prxs were found to interact with proteins involved in protein folding (Cerveau et al., 2016). Therefore, the activity of the NTRC-2-Cys Prxs system may affect protein import to chloroplasts, supporting the notion that import of preproteins is regulated by the redox status of the organelle (Balseira et al., 2010). In line with this possibility, HSP70-4, but also HSP90-1, induced in both *2cpab* and *ntrc-2cpab* (Supplemental Appendix S1 and Supplemental Table S1), were shown to accumulate in the *Arabidopsis* double mutant deficient in GENOMES UNCOUPLED 1 (GUN1) and CLIP PROTEASE C1 (CLPC1), chloroplast proteins involved in plastid-to-nucleus retrograde signaling and protein import, respectively (Wu et al., 2019). In this regard, it is worth mentioning that 2-Cys Prx, but not NTRC, was identified among the interactors of GUN1 in developing seedlings (Wu et al., 2019), raising the possibility that these enzymes might be functionally related, most likely in an NTRC-independent manner; however, the putative role of 2-Cys Prxs in retrograde signaling is yet unknown. As mentioned above, the albino/variegated cotyledons phenotype of *2cpab* and *ntrc-2cpab* seedlings (Figure 2) indicates defective chloroplast biogenesis in these mutants. Since this phenotype is exclusive to the *2cpab* and *ntrc-2cpab* mutants, but not the *ntrc* mutant, the function of 2-Cys Prxs in chloroplast biogenesis seems to be NTRC-independent. Therefore, the induction of HSP70-4 and HSP90-1 at both the transcript (Figure 7A; Supplemental Table S1) and protein levels (Figure 7B and C) in the *2cpab* and *ntrc-2cpab* mutants suggests that the NTRC-2-Cys Prxs redox system might influence protein import to fully developed chloroplasts, which may have dramatic effects on chloroplast biogenesis at early stages of development.

In summary, the results presented in this study support the notion that the most relevant function of NTRC is the control of the redox state of 2-Cys Prxs in fully developed chloroplasts. Since NTRC interacts with targets other than 2-Cys Prxs, additional functions of the NTRC via the direct interaction with these targets cannot be ruled out and may be complementary with the role of the enzyme in 2-Cys Prxs regulation. The catalytic cycle of 2-Cys Prx, which implies the use of thiol reducing equivalents (from NTRC and Trxs) to reduce hydrogen peroxide, allows the function of this enzyme to interconnect redox regulation with antioxidant mechanisms via its contribution to the water–water cycle, allowing the rapid control of chloroplast redox regulated processes in response to changes in light intensity and during the day–night transition. Finally, the comparative transcriptomic analysis of the *2cpab* and *ntrc-2cpab* mutants highly suggests the participation of the NTRC-2-Cys Prxs system in protein quality control outside the organelle. This function may be especially relevant in chloroplast biogenesis

at early stages of plant development, as suggested by the aberrant cotyledon phenotypes of the *2cpab* and *ntrc-2cpab* mutants. Interestingly, the *ntrc* mutant does not show albino cotyledon phenotype, indicating NTRC-independent functions for 2-Cys Prxs, yet unknown, at early stages of development.

Materials and methods

Biological material and growth conditions

Arabidopsis (*Arabidopsis thaliana*) wild-type (ecotype Columbia) and mutant plants (Supplemental Table S2) were routinely grown in soil in growth chambers. Tested photoperiods were long-day (16-h light/8-h darkness), short-day (8-h light/16-h darkness) and ultra-short-day (4-h light/20-h darkness) at 22°C and 20°C during light and dark periods, respectively, and light intensity of 125 $\mu\text{E m}^{-2} \text{s}^{-1}$ unless otherwise specified. To generate the *ntrc-2cpab* triple mutant, the previously described *ntrc* (Serrato et al., 2004) and *2cpab* (Ojeda et al., 2018a) mutants were manually crossed and the triple homozygous line was identified in the progeny by PCR analysis of genomic DNA with oligonucleotides listed in Supplemental Table S3.

Cotyledon phenotype analyses were performed on seedlings grown on Murashige and Skoog medium containing 0.35% (w/v) Gelrite (Duchefa) and 0.5% (w/v) sucrose. In brief, sets of at least 50 seeds of the different lines under analysis were sown on plates and grown under continuous light. The cotyledon phenotypes, grouped as green, albino or pale/variegated/asymmetric, were scored at 7 d to determine the percentage of seedlings within each group.

Protein extraction, alkylation assays, and western blot analysis

Plant tissues were ground under liquid nitrogen to a fine powder. Extraction buffer (50 mM Tris–HCl, pH 8.0, 0.15 M NaCl, 0.5% (v/v) Nonidet P-40) was immediately added, mixed on a vortex and centrifuged at 16,100g at 4°C for 20 min. Protein was quantified using the Bradford reagent (Bio-Rad). Alkylation assays were performed as previously described (Pérez-Ruiz et al., 2017) using 10 mM MM-PEG₂₄ or 60 mM IAA as indicated. Protein samples were subjected to sodium dodecyl sulphate-polyacrylamide gel electrophoresis (SDS–PAGE) under reducing (NTRC, 2-Cys Prxs, HSP70, and HSP90-1) or nonreducing (FBPase, PRK, RCA, ATPc, and Trxs *f*) conditions using acrylamide gel concentration of 9.5% (FBPase, PRK, RCA, and ATPc), 12% (NTRC, 2-Cys Prxs, HSP70, and HSP90-1), and 15% (Trxs *f*). Resolved proteins were transferred to nitrocellulose membranes and probed with the indicated antibody. Specific antibodies for NTRC (Serrato et al., 2004), 2-Cys Prxs (Pérez-Ruiz et al., 2006), and Trxs *f* (Naranjo et al., 2016b) were previously raised in our laboratory. The anti-FBPase and anti-RCA antibodies were kindly provided by Dr Sahrawy (Estación Experimental del Zaidín, Granada, Spain) and Dr A. R. Portis (USDA, Urbana, USA), respectively. Antibodies

for ATPc, PRK, HSP70, and HSP90-1 were purchased from Agrisera (Sweden).

Determination of chlorophyll levels, measurements of chlorophyll *a* fluorescence, and determination of carbon assimilation rates

Chlorophyll levels were measured as previously described (Pérez-Ruiz et al., 2006). Room temperature chlorophyll fluorescence was measured using a pulse–amplitude modulation fluorometer (DUAL-PAM-100; Walz). The maximum quantum yield of PSII was assayed after incubation of plants in the dark for 30 min by calculating the ratio of the variable fluorescence, F_v , to maximal fluorescence, F_m (F_v/F_m). Induction–recovery curves were performed using red (635 nm) actinic light at $75 \mu\text{E m}^{-2} \text{s}^{-1}$ for 8 min. Saturating pulses of red light at $10,000 \mu\text{E m}^{-2} \text{s}^{-1}$ intensity and 0.6 s duration were applied every 60 s and recovery in darkness was recorded for up to 10 min. The parameters $Y(\text{II})$ and $Y(\text{NPQ})$, corresponding to the respective quantum yields of PSII photochemistry and nonregulated basal quenching, were calculated according to reported equations (Kramer et al., 2004). Measurements of relative linear ETRs (II) were based on chlorophyll fluorescence of pre-illuminated plants by applying stepwise increasing actinic light intensities up to $344 \mu\text{E m}^{-2} \text{s}^{-1}$. Net CO_2 assimilation rate (A_N) was measured as previously reported (Ojeda et al., 2017), using an open gas exchange system Li-6400 equipped with the chamber head (Li-6400–40) in dark-adapted leaves of plants grown under short-day for 8 weeks. Measurements were performed by the Service for Photosynthesis, Instituto de Recursos Naturales y Agrobiología de Sevilla (Spain).

Transcriptomic Analysis by RNA-Seq and RT-qPCR

Eight-week-old short-day grown wild-type, *2cpab*, and *ntrc-2cpab* plants were randomly selected and young rosette leaves collected after 2 h of illumination at $125 \mu\text{E m}^{-2} \text{s}^{-1}$. Our experimental design consisted of three biological replicates for each genotype, each of them containing leaves from three individual plants. RNA extraction was performed from pooled leaf samples using Sure Prep kit (Fisher), following the manufacturer's instructions. RNA concentration and purity were tested by an Agilent 2100 Bioanalyzer, a microfluidics-based platform that performs quality control of DNA and RNA samples before sequencing. Library construction of cDNA molecules was carried out following the manufacturer's instructions using the TruSeq Stranded Total RNA with Ribo-Zero kit (Illumina). The generated DNA fragments were sequenced with the Illumina HiSeq 4000 platform, yielding approximately 60–80 million 150-bp long paired-end reads for each sample. Quality control was carried out using the software package FastQC (<http://www.bioinformatics.babraham.ac.uk/projects/fastqc/>) confirming that all samples were of good quality. No preprocessing of the reads was required to trim low-quality read fragments. The Arabidopsis Col-0 TAIR 10 reference genome was downloaded from the Ensembl Plants Database ([\[ensembl.org/\]\(http://ensembl.org/\)\). Read mapping to the reference genome and transcript assembly were performed with the software tools HISAT2 and StringTie \(Pertea et al., 2016\) using default parameters. Differential expression analysis was carried out with the Bioconductor R packages Ballgown \(Pertea et al., 2016\) and LIMMA \(Ritchie et al., 2015\) using a fold change of \$\pm \log_2\(2\)\$ and \$P < 0.05\$ computed according to a moderated \$t\$ test. The R package VennDiagram was used to generate Venn diagrams comparing the different sets of DEGs. GO term and KEGG pathways enrichment analysis over the different gene sets was performed with the Bioconductor R package ClusterProfiler \(Yu et al., 2012\). Subcellular distribution of proteins encoded by DEGs was assigned according to the SUBcellular Arabidopsis consensus \(SUBAcon\) algorithm \(<http://suba.live/>; Hooper et al., 2017\). Principal component analysis and hierarchical clustering was carried out using the R Packages FactoMineR \(Le et al., 2008\). Heatmaps representing gene expression fold-changes in the mutants with respect to the wild-type were generated using the function heatmap.2 from the R package gplots. Gene members of the HSP20, HSP70, and HSP90 are classified according to Swindell et al. \(2007\) and listed in Supplementary Table S4. For RT-qPCR analysis, total RNA was extracted using Trizol reagent \(Invitrogen\) and cDNA synthesis was performed with 1 \$\mu\text{g}\$ of total RNA using the Maxima first-strand cDNA synthesis kit \(Thermo Scientific\) according to manufacturer's instructions. Real-time quantitative PCR \(RT-qPCR\) was performed using an IQ5 real-time PCR detection system \(Bio-Rad\). Oligonucleotides used for RT-qPCR analyses are listed in Supplementary Table S3. Expression levels were normalized using *ACTIN2* and *UBQ10* as reference genes.](https://plants.</p>
</div>
<div data-bbox=)

Accession numbers

The RNA-seq data sets generated in this study have been deposited in the Gene Expression Omnibus (GEO) under accession GSE147793.

Supplemental data

The following materials are available in the online version of this article.

Supplemental Figure S1. The phenotype of the Arabidopsis WT and mutants *ntrc*, *2cpab* and *ntrc-2cpab* grown under long-day photoperiod.

Supplemental Figure S2. Effect of prolonged nights and different light intensities on the growth of the Arabidopsis WT and mutants *ntrc*, *2cpab*, and *ntrc-2cpab*.

Supplemental Figure S3. In vivo redox state of Trxs *f* in WT and mutants *ntrc*, *2cpab*, and *ntrc-2cpab* in response to light.

Supplemental Figure S4. Correlation between the transcriptomes of the three biological replicates per Arabidopsis line.

Supplemental Figure S5. Subcellular distribution of proteins encoded by DEGs in the *2cpab* and *ntrc-2cpab* mutants.

Supplemental Figure S6. Principal component analysis of global gene expression.

Supplemental Figure S7. Genes specifically activated in the *ntrc-2cpab* mutant.

Supplemental Figure S8. Genes specifically repressed in the *ntrc-2cpab* mutant.

Supplemental Figure S9. RT-qPCR analysis of selected genes specifically upregulated or downregulated in the *ntrc-2cpab* mutant.

Supplemental Figure S10. GO enrichment analysis of upregulated genes in *2cpab* and *ntrc-2cpab* mutants.

Supplemental Figure S11. GO enrichment analysis of downregulated genes in the *ntrc-2cpab* mutant.

Supplemental Figure S12. RT-qPCR analysis of selected genes commonly upregulated or downregulated in the *2cpab* and *ntrc-2cpab* mutants.

Supplemental Figure S13. Heat-map analysis of the differential expression of chaperone encoding genes of the HSP20, HSP70 and HSP90 families in the *2cpab* and *ntrc-2cpab* mutants.

Supplemental Appendix S1. DEGs in the *2cpab* and *ntrc-2cpab* mutant lines.

Supplemental Appendix S2. GO term enrichment in the *2cpab* and *ntrc-2cpab* mutant lines.

Supplemental Table S1. Commonly DEGs in the *2cpab* and *ntrc-2cpab* mutants.

Supplemental Table S2. *Arabidopsis* mutants used in this study.

Supplemental Table S3. Oligonucleotides used in this study.

Supplemental Table S4. Members of the HSP20, HSP70 and HSP90 gene families from *Arabidopsis thaliana*.

Acknowledgments

V.O. was recipient of a pre-doctoral fellowship from Spanish Ministry of Innovation and Competitiveness, J.J.L. received a contract from Junta de Andalucía (Spain). The anti-FBPase and anti-RCA antibodies were kindly provided by Dr M. Sahrawy, Estación Experimental del Zaidín, Granada, Spain and Dr A. R. Portis, USDA, Urbana, USA, respectively.

Funding

This work was supported by European Regional Development Fund-cofinanced grant (BIO2017-85195-C2-1-P) from the Spanish Ministry of Innovation and Competitiveness (MINECO).

Conflict of interest statement: Authors declare no conflict of interest.

References

- Alkhalfioui F, Renard M, Montrichard F (2007) Unique properties of NADP-thioredoxin reductase C in legumes. *J Exp Bot* **58**: 969–978
- Aviezer-Hagai K, Skovorodnikova J, Galigniana M, Farchi-Pisanty O, Maayan E, Bocovza S, Efrat Y, von Koskull-Döring P, Ohad N, Breiman A (2007) *Arabidopsis* immunophilins ROF1 (AtFKBP62) and ROF2 (AtFKBP65) exhibit tissue specificity, are heat-stress induced, and bind HSP90. *Plant Mol Biol* **63**: 237–255
- Awad J, Stotz H, Fekete A, Krischke M, Engert C, Havaux M, Berger S, Mueller MJ (2015) 2-cysteine peroxiredoxins and thylakoid ascorbate peroxidase create a water-water cycle that is essential to protect the photosynthetic apparatus under high light stress conditions. *Plant Physiol* **167**: 1592–1603
- Baier M, Noctor G, Foyer CH, Dietz KJ (2000) Antisense suppression of 2-cysteine peroxiredoxin in *Arabidopsis* specifically enhances the activities and expression of enzymes associated with ascorbate metabolism but not glutathione metabolism. *Plant Physiol* **124**: 823–832
- Balsera M, Soll J, Buchanan BB (2010) Redox extends its regulatory reach to chloroplast protein import. *Trends Plant Sci* **15**: 515–521
- Balsera M, Buchanan BB (2019) Evolution of the thioredoxin system as a step enabling adaptation to oxidative stress. *Free Radic Biol Med* **140**: 28–35
- Bernal-Bayard P, Hervás M, Cejudo FJ, Navarro JA (2012) Electron transfer pathways and dynamics of chloroplast NADPH-dependent thioredoxin reductase C (NTRC). *J Biol Chem* **287**: 33865–33872
- Bernal-Bayard P, Ojeda V, Hervás M, Cejudo FJ, Navarro JA, Velázquez-Campoy A, Pérez-Ruiz JM (2014) Molecular recognition in the interaction of chloroplast 2-Cys peroxiredoxin with NADPH-thioredoxin reductase C (NTRC) and thioredoxin x. *FEBS Lett* **588**: 4342–4347
- Böhrer AS, Massot V, Innocenti G, Reichheld JP, Issakidis-Bourguet E, Vanacker H (2012) New insights into the reduction systems of plastidial thioredoxins point out the unique properties of thioredoxin z from *Arabidopsis*. *J Exp Bot* **63**: 6315–6323
- Broin M, Cuine S, Eymery F, Rey P (2002) The plastidic 2-cysteine peroxiredoxin is a target for a thioredoxin involved in the protection of the photosynthetic apparatus against oxidative damage. *Plant Cell* **14**: 1417–1432
- Carrillo LR, Froehlich JE, Cruz JA, Savage L, Kramer DM (2016) Multi-level regulation of the chloroplast ATP synthase: The chloroplast NADPH thioredoxin reductase C (NTRC) is required for redox modulation specifically under low irradiance. *Plant J* **87**: 654–663
- Cejudo FJ, Ojeda V, Delgado-Requeray V, González M, Pérez-Ruiz JM (2019) Chloroplast redox regulatory mechanisms in plant adaptation to light and darkness. *Front Plant Sci* **10**: 380
- Cejudo FJ, González M, Pérez-Ruiz JM (2021) Redox regulation of chloroplast metabolism. *Plant Physiol* **186**: 9–21
- Cerveau D, Kraut A, Stotz HU, Mueller MJ, Coute Y, Rey P (2016) Characterization of the *Arabidopsis thaliana* 2-Cys peroxiredoxin interactome. *Plant Sci* **252**: 30–41
- Cheng F, Zhou Y-H, Xia X-J, Shi K, Zhou J, Yu J-Q (2014) Chloroplastic thioredoxin-f and thioredoxin-m1/4 play important roles in brassinosteroids-induced changes in CO₂ assimilation and cellular redox homeostasis in tomato. *J Exp Bot* **65**: 4335–4347
- Chae HB, Moon JC, Shin MR, Chi YH, Jung YJ, Lee SY, Nawkar GM, Jung HS, Hyun JK, Kim WY, et al. (2013) Thioredoxin reductase type C (NTRC) orchestrates enhanced thermotolerance to *Arabidopsis* by its redox-dependent holdase chaperone function. *Mol Plant* **6**: 323–336
- Collin V, Issakidis-Bourguet E, Marchand C, Hirasawa M, Lancelin J-M, Knaff DB, Miginiac-Maslow M (2003) The *Arabidopsis* plastidial thioredoxins: new functions and new insights into specificity. *J Biol Chem* **278**: 23747–23752
- Courteille A, Vesa S, Sanz-Barrio R, Cazale AC, Becuwe-Linka N, Farran I, Havaux M, Rey P, Rumeau D (2013) Thioredoxin m4 controls photosynthetic alternative electron pathways in *Arabidopsis*. *Plant Physiol* **161**: 508–520
- Dangoor I, Peled-Zehavi H, Wittenberg G, Danon A (2012) A chloroplast light-regulated oxidative sensor for moderate light intensity in *Arabidopsis*. *Plant Cell* **24**: 1894–1906
- Dietz KJ (2011) Peroxiredoxins in plants and cyanobacteria. *Antioxid Redox Signal* **15**: 1129–1159

- Eliyahu E, Rog I, Inbal D, Danon A** (2015) ACHT4-driven oxidation of APS1 attenuates starch synthesis under low light intensity in Arabidopsis plants. *Proc Natl Acad Sci U S A* **112**: 12876–12881
- Foyer C, Furbank R, Harbinson J, Horton P** (1990) The mechanisms contributing to photosynthetic control of electron transport by carbon assimilation in leaves. *Photosynth Res* **25**: 83–100
- Geigenberger P, Thormählen I, Daloso DM, Fernie AR** (2017) The unprecedented versatility of the plant thioredoxin system. *Trends Plant Sci* **22**: 249–262
- González M, Delgado-Requerey V, Ferrández J, Serna A, Cejudo FJ** (2019) Insights into the function of NADPH thioredoxin reductase C (NTRC) based on identification of NTRC-interacting proteins in vivo. *J Exp Bot* **70**: 5787–5798
- Hochmal AK, Zinzius K, Charoenwattanasatien R, Gäbelein P, Mutoh R, Tanaka H, Schulze S, Liu G, Scholz M, Nordhues A, et al.** (2016) Calredoxin represents a novel type of calcium-dependent sensor-responder connected to redox regulation in the chloroplast. *Nat Commun* **7**: 11847
- Hooper CM, Castleden IR, Tanz SK, Aryamanesh N, Millar AH** (2017) SUBA4: the interactive data analysis centre for Arabidopsis subcellular protein locations. *Nucl Acids Res* **45**: D1064–D1074
- Ishiga Y, Ishiga T, Ikeda Y, Matsuura T, Mysore KS** (2016) NADPH-dependent thioredoxin reductase C plays a role in nonhost disease resistance against *Pseudomonas syringae* pathogens by regulating chloroplast-generated reactive oxygen species. *PeerJ* **4**: e1938
- Ishiga Y, Ishiga T, Wangdi T, Mysore KS, Uppalapati SR** (2012) NTRC and chloroplast-generated reactive oxygen species regulate *Pseudomonas syringae* pv. tomato disease development in tomato and Arabidopsis. *Mol Plant-Microb Interact* **25**: 294–306
- Jacquot JP, Eklund H, Rouhier N, Schürmann P** (2009) Structural and evolutionary aspects of thioredoxin reductases in photosynthetic organisms. *Trends Plant Sci* **14**: 336–343
- Jurado-Flores A, Delgado-Requerey V, Gálvez-Ramírez A, Puerto-Galán L, Pérez-Ruiz JM, Cejudo FJ** (2020) Exploring the functional relationship between γ -type thioredoxins and 2-Cys peroxiredoxins in Arabidopsis chloroplasts. *Antioxidants* **9**: 1072
- Kirchsteiger K, Ferrández J, Pascual MB, González M, Cejudo FJ** (2012) NADPH thioredoxin reductase C is localized in plastids of photosynthetic and nonphotosynthetic tissues and is involved in lateral root formation in Arabidopsis. *Plant Cell* **24**: 1534–1548
- Kramer DM, Johnson G, Kiirats O, Edwards GE** (2004) New fluorescence parameters for the determination of $q(a)$ redox state and excitation energy fluxes. *Photosynth Res* **79**: 209–218
- Le S, Josep J, Huson F** (2008) FactoMineR: A package for multivariate analysis. *J Stat Softw* **25**: 1–18
- Lee S, Lee DW, Lee Y, Mayer U, Stierhof YD, Lee S, Jurgens G, Hwang I** (2009) Heat shock protein cognate 70-4 and an E3 ubiquitin ligase, CHIP, mediate plastid-destined precursor degradation through the ubiquitin-26S proteasome system in Arabidopsis. *Plant Cell* **21**: 3984–4001
- Lepistö A, Pakula E, Toivola J, Krieger-Liszkay A, Vignols F, Rintamäki E** (2013) Deletion of chloroplast NADPH-dependent thioredoxin reductase results in inability to regulate starch synthesis and causes stunted growth under short-day photoperiods. *J Exp Bot* **64**: 3843–3854
- Littlejohn GR, Breen S, Smirnoff N, Grant M** (2021) Chloroplast immunity illuminated. *New Phytol* **229**: 3088–3107
- Machida T, Ishibashi A, Kirino A, Sato J-I, Kawasaki S, Niimura Y, Honjoh K-I, Miyamoto T** (2012) Chloroplast NADPH-dependent thioredoxin reductase from *Chlorella vulgaris* alleviates environmental stresses in yeast together with 2-Cys peroxiredoxin. *PLoS One* **7**: e45988
- Michalska J, Zauber H, Buchanan BB, Cejudo FJ, Geigenberger P** (2009) NTRC links built-in thioredoxin to light and sucrose in regulating starch synthesis in chloroplasts and amyloplasts. *Proc Natl Acad Sci U S A* **106**: 9908–9913
- Mihara S, Yoshida K, Higo A, Hisabori T** (2017) Functional significance of NADPH-thioredoxin reductase C in the antioxidant defense system of cyanobacterium *Anabaena* sp. PCC 7120. *Plant Cell Physiol* **58**: 86–94
- Moon JC, Jang HH, Chae HB, Lee JR, Lee SY, Jung YJ, Shin MR, Lim HS, Chung WS, Yun DJ, et al.** (2006) The C-type Arabidopsis thioredoxin reductase ANTR-C acts as an electron donor to 2-Cys peroxiredoxins in chloroplasts. *Biochem Biophys Res Commun* **348**: 478–484
- Montillet J-L, Rondet D, Brugière S, Henri P, Rumeau D, Reichheld J-P, Couté Y, Leonhardt L, Rey P** (2021) Plastidial and cytosolic thiol reductases participate in the control of stomatal functioning. *Plant Cell Environ* **44**: 1417–1435
- Moon JC, Jang HH, Chae HB, Lee JR, Lee SY, Jung YJ, Shin MR, Lim HS, Chung WS, Yun DJ, Lee KO** (2006) The C-type Arabidopsis thioredoxin reductase ANTR-C acts as an electron donor to 2-Cys peroxiredoxins in chloroplasts. *Biochem Biophys Res Commun* **348**: 478–484
- Naranjo B, Migné C, Krieger-Liszkay A, Hornero-Méndez D, Gallardo-Guerrero L, Cejudo FJ, Lindahl M** (2016a) The chloroplast NADPH thioredoxin reductase C, NTRC, controls non-photochemical quenching of light energy and photosynthetic electron transport in Arabidopsis. *Plant Cell Environ* **39**: 804–822
- Naranjo B, Díaz-Espejo A, Lindahl M, Cejudo FJ** (2016b) Type f thioredoxins have a role in the short-term activation of carbon metabolism and their loss affects growth under short-day conditions in Arabidopsis thaliana. *J Exp Bot* **67**: 1951–1964
- Nikkanen L, Toivola J, Rintamäki E** (2016) Crosstalk between chloroplast thioredoxin systems in regulation of photosynthesis. *Plant Cell Environ* **39**: 1691–1705
- Nikkanen L, Rintamäki E** (2019) Chloroplast thioredoxin systems dynamically regulate photosynthesis in plants. *Biochem J* **476**: 1159–1172
- Ojeda V, Pérez-Ruiz JM, González M, Nájera VA, Sahrawy M, Serrato AJ, Geigenberger P, Cejudo FJ** (2017) NADPH thioredoxin reductase C and thioredoxins act concertedly in seedling development. *Plant Physiol* **174**: 1436–1448
- Ojeda V, Pérez-Ruiz JM, Cejudo FJ** (2018a) 2-Cys Peroxiredoxins participate in the oxidation of chloroplast enzymes in the dark. *Mol Plant* **11**: 1377–1388
- Ojeda V, Pérez-Ruiz JM, Cejudo FJ** (2018b) The NADPH-dependent thioredoxin reductase C-2-Cys peroxiredoxin redox system modulates the activity of thioredoxin x in Arabidopsis chloroplasts. *Plant Cell Physiol* **59**: 2155–2164
- Okegawa Y, Motohashi K** (2020) M-type thioredoxins regulate the PGR5/PGR1-dependent pathway by forming a disulfide-linked complex with PGR1. *Plant Cell* **32**: 3866–3883
- Pérez-Ruiz JM, Spínola MC, Kirchsteiger K, Moreno J, Sahrawy M, Cejudo FJ** (2006) Rice NTRC is a high-efficiency redox system for chloroplast protection against oxidative damage. *Plant Cell* **18**: 2356–2368
- Pérez-Ruiz JM, Cejudo FJ** (2009) A proposed reaction mechanism for rice NADPH thioredoxin reductase C, an enzyme with protein disulfide reductase activity. *FEBS Lett* **583**: 1399–1402
- Pérez-Ruiz JM, Guinea M, Puerto-Galán L, Cejudo FJ** (2014) NADPH thioredoxin reductase C is involved in redox regulation of the Mg-chelatase I subunit in Arabidopsis thaliana chloroplasts. *Mol Plant* **7**: 1252–1255
- Pérez-Ruiz JM, Naranjo B, Ojeda V, Guinea M, Cejudo FJ** (2017) NTRC-dependent redox balance of 2-Cys peroxiredoxins is needed for optimal function of the photosynthetic apparatus. *Proc Natl Acad Sci U S A* **114**: 12069–12074
- Pertea M, Kim D, Pertea G, Leek JT, Salzberg SL** (2016) Transcript-level expression analysis of RNA-seq experiments with HISAT, StringTie and Ballgown. *Nat Protoc* **11**: 1650–1667
- Pulido P, Spínola C, Kirchsteiger K, Guinea M, Pascual MB, Sahrawy M, Sandalio LM, Dietz K-J, González M, Cejudo FJ** (2010) Functional analysis of the pathways for 2-Cys peroxiredoxin

- reduction in *Arabidopsis thaliana* chloroplasts. *J Exp Bot* **61**: 4043–4054
- Richter AS, Peter E, Rothbart M, Schlicke H, Toivola J, Rintamäki E, Grimm B** (2013) Posttranslational influence of NADPH-dependent thioredoxin reductase C on enzymes of tetrapyrrole synthesis. *Plant Physiol* **162**: 63–73
- Ritchie ME, Phipson B, Wu D, Hu Y, Law CW, Shi W, Smyth GK** (2015) Limma powers differential expression analyses for RNA-sequencing and microarray studies. *Nucleic Acids Res* **43**: e47
- Sánchez-Riego AM, Mata-Cabana A, Galmozzi CV, Florencio FJ** (2016) NADPH-thioredoxin reductase C mediates the response to oxidative stress and thermotolerance in the cyanobacterium *Anabaena* sp. PCC7120. *Front Microbiol* **7**: 1283
- Serrato AJ, Pérez-Ruiz JM, Spínola MC, Cejudo FJ** (2004) A novel NADPH thioredoxin reductase, localized in the chloroplast, which deficiency causes hypersensitivity to abiotic stress in *Arabidopsis thaliana*. *J Biol Chem* **279**: 43821–43827
- Schürmann P, Buchanan BB** (2008) The ferredoxin/thioredoxin system of oxygenic photosynthesis. *Antioxid Redox Signal* **10**: 1235–1274
- Stenbaek A, Hansson A, Wulff RP, Hansson M, Dietz K-J, Jensen PE** (2008) NADPH-dependent thioredoxin reductase and 2-Cys peroxiredoxins are needed for the protection of Mg-protoporphyrin monomethyl ester cyclase. *FEBS Lett* **582**: 2773–2778
- Swindell WR, Huebner M, Weber AP** (2007) Transcriptional profiling of *Arabidopsis* heat shock proteins and transcription factors reveals extensive overlap between heat and non-heat stress response pathways. *BMC Genomics* **8**: 125
- Toivola J, Nikkanen L, Dahlström KM, Salminen TA, Lepistö A, Vignols HF, Rintamäki E** (2013) Overexpression of chloroplast NADPH-dependent thioredoxin reductase in *Arabidopsis* enhances leaf growth and elucidates in vivo function of reductase and thioredoxin domains. *Front Plant Sci* **4**: 389
- Thormählen I, Meitzel T, Groysman J, Öchsner AB, von Roepenack-Lahaye E, Naranjo B, Cejudo FJ, Geigenberger P** (2015) Thioredoxin f1 and NADPH-dependent thioredoxin reductase C have overlapping functions in regulating photosynthetic metabolism and plant growth in response to varying light conditions. *Plant Physiol* **169**: 1766–1786
- Vaseghi MJ, Chibani K, Telman W, Liebthal M, Gerken M, Schnitzer H, Müller S, Dietz K-J** (2018) The chloroplast 2-cysteine peroxiredoxin functions as thioredoxin oxidase in redox regulation of chloroplast metabolism. *eLife* **7**: e38194
- Wu GZ, Meyer EH, Richter AS, Schuster M, Ling Q, Schottler MA, Walther D, Zoschke R, Grimm B, Jarvis RP, Bock R** (2019) Control of retrograde signalling by protein import and cytosolic folding stress. *Nat Plants* **5**: 525–538
- Yoshida K, Hisabori T** (2016) Two distinct redox cascades cooperatively regulate chloroplast functions and sustain plant viability. *Proc Natl Acad Sci U S A* **113**: E3967–E3976
- Yoshida K, Hara A, Sugiura K, Fukaya Y, Hisabori T** (2018) Thioredoxin-like2/2-Cys peroxiredoxin redox cascade supports oxidative thiol modulation in chloroplasts. *Proc Natl Acad Sci U S A* **115**: E8296–E8304
- Yoshida K, Yokochi Y, Hisabori T** (2019) New light on chloroplast redox regulation: molecular mechanism of protein thiol oxidation. *Front Plant Sci* **10**: 1534
- Yu G, Wang L, Han Y, He Q** (2012) clusterProfiler: an R package for comparing biological themes among gene clusters. *OMICS: J Int Biol* **16**: 284–287
- Zaffagnini M, Fermani S, Marchand CH, Costa A, Sparla F, Rouhier N, Geigenberger P, Lemaire SD, Trost P** (2019) Redox homeostasis in photosynthetic organisms: novel and established thiol-based molecular mechanisms. *Antioxid Redox Signal* **31**: 155–210